

Chaos at the rim of black hole and fuzzball shadows

M. Bianchi,^{a,b} A. Grillo,^{a,b} J.F. Morales^b

^a*Dipartimento di Fisica, Università di Roma “Tor Vergata”,
Via della Ricerca Scientifica, 00133 Roma, Italy*

^b*I.N.F.N. Sezione di Roma “Tor Vergata”,
Via della Ricerca Scientifica, 00133 Roma, Italy*

E-mail: massimo.bianchi@roma2.infn.it, morales@roma2.infn.it,
alfredo.grillo@roma2.infn.it

ABSTRACT: We study the scattering of massless probes in the vicinity of the *photon-sphere* of asymptotically AdS black holes and horizon-free microstate geometries (fuzzballs). We find that these exhibit a chaotic behaviour characterised by exponentially large deviations of nearby trajectories. We compute the Lyapunov exponent λ governing the exponential growth in d dimensions and show that it is bounded from above by $\lambda_b = \sqrt{d-3}/2b_{\min}$ where b_{\min} is the minimal impact parameter under which a massless particle is swallowed by the black hole or gets trapped in the fuzzball for a very long time. Moreover we observe that λ is typically below the advocated bound on chaos $\lambda_H = 2\pi\kappa_B T/\hbar$, that in turn characterises the radial fall into the horizon, but the bound is violated in a narrow window near extremality, where the photon-sphere coalesces with the horizon. Finally, we find that fuzzballs are characterised by Lyapunov exponents smaller than those of the corresponding BH's suggesting the possibility of discriminating the existence of microstructures at horizon scales via the detection of ring-down modes with time scales λ^{-1} longer than those expected for a BH of the given mass and spin.

KEYWORDS: Black holes, fuzzballs, chaos, geodesics, holography

Contents

1	Introduction	1
2	Geodesics on AdS Kerr-Newman space-times	4
2.1	The metric	4
2.2	The Hamiltonian and momenta	4
2.3	Motion in the radial direction	6
2.4	Motion in the θ direction	7
2.5	Geodesics inside the absorption region	9
3	Critical and nearly critical geodesics	10
3.1	Critical geodesics	10
3.2	The Lyapunov exponent	11
4	Analytic results for specific BH's	13
4.1	Non rotating BH's in AdS	13
4.2	Rotating BH's	15
4.3	Spherical symmetric BH's in higher dimensions	16
5	Fuzzball geometries	17
5.1	The BH geometry	18
5.2	The asymptotically flat fuzzball	19
5.3	Asymptotically AdS geometry	20
6	Discussion and outlook	21
A	Integrating the angular motion	23

1 Introduction

A light ray travelling near a massive object gets deflected and delayed with respect to its propagation in flat space-time. If the massive object is a black hole (BH), the time delay and angular deflection, that are small at large impact parameter, can get arbitrarily large at some critical value. For critical impact parameters even light gets trapped in (unstable) ‘circular’¹ orbits around the BH. Below this critical threshold no signal can escape from the BH gravitational potential.

The limiting ‘circular’ photon orbits form the BH *photon-sphere* that discriminates between the scattering and absorption regimes. It appears as the rim of the *black hole*

¹We put ‘circular’ in quotes, since closed geodesics at constant ‘radial’ variable in a curved geometry are not necessarily circles.

shadow projected by the BH on a distant observer. The size and shape of the photon-sphere depends on the mass, charge and angular momentum of the BH and can help to uniquely identify it. For instance, for a Schwarzschild BH the photon-sphere is a sphere of radius $3/2$ times that of the BH horizon². Photon orbits are also useful to explain the optical appearance of stars undergoing gravitational collapse and the response of the BH to perturbations, the so called quasi-normal modes, that can be interpreted as null particles trapped at the unstable orbit and slowly leaking out [2].

Instability of the photon orbits signals the onset of chaos on the geodesic motion near the photon-sphere [2]. A measure of chaos or, better, of the high sensitivity to the initial conditions is given by the Lyapunov exponent λ , that can be defined via the Poisson bracket

$$\{\phi(0), \phi(t)\}_{\text{P.B.}} = \frac{\delta\phi(t)}{\delta P_\phi} \sim e^{\lambda t} \quad (1.1)$$

describing the exponential growth with time of the deflection along an angular direction ϕ , for small variations of the corresponding conjugate momentum P_ϕ . In the case of spherically symmetric BH's, the Lyapunov exponent λ can be related to the time decay of the basic QNM [2]. In an asymptotically AdS space, the chaotic behaviour manifests as a random angular dispersion of nearby trajectories re-emerging at the boundary after a long time t , much longer than the time it takes for a free massless particle to travel from/to the boundary and back.

Our work is inspired by the results in [3], where holography was used to diagnose chaos in quantum mechanical systems at finite temperature. The amount of chaos in the quantum theory was characterised by the exponential growth of out-of-time-ordered correlators, involving commutators that replace the Poisson brackets in (1.1) and encode the perturbation induced by an operator on a later measurement. The long time behaviour of the field theory correlator was related to the exponential growth $e^{\lambda_H t}$ of the center-of-mass energy of the high energy scattering process in the dual gravity theory [4, 5]. The exponent $\lambda_H = 2\pi\kappa_B T/\hbar$, with T the temperature of the BH, is known to be determined by the local Rindler structure of the horizon [6] and it was proposed as a universal bound on the chaos that a quantum thermal system can develop [3].

In this paper we compute the Lyapunov exponent for scattering near the photon-sphere of asymptotically AdS charged rotating BH's in $d = 4$ and, later on, generalise our analysis to diverse dimensions d and to horizon-free micro-state geometries a.k.a. *fuzzballs* [7–10]. We relate the Lyapunov exponent λ to the vanishing rate of the radial velocity $\dot{r} \approx -2\lambda(r - r_c)$ near the photon-sphere, and derive analytic formulae for λ as a function of the radius r_c of the limiting photon orbit.

We find that λ is typically smaller than λ_H characterising the vanishing rate of the radial velocity at the horizon³, but the bound is violated inside a very narrow window near

²We observe that this radius is larger than the ‘‘Buchdahl bound’’ $R_B = \frac{9}{8}r_H$, i.e. the outermost radius of stability for a fluid sphere made of ‘conventional’ matter [1], so in principle even a star (more likely a cold neutron star than a hot star like our sun) can have a photon-sphere (not to be confused with the ‘photo-sphere’).

³Our definition of λ differs from that of [2] by a factor of 2. Our normalization is chosen so that λ_H matches the Lyapunov exponent of the near horizon boundary theory.

extremality when the innermost region of the BH photon-sphere coalesces with the BH horizon⁴.

We find⁵ instead that

$$\lambda \leq \lambda_b = \frac{\sqrt{d-3}}{2b_{\min}} \quad (1.2)$$

with d the dimension and b_{\min} the minimal impact parameter under which a particle moving in the background of the BH gets trapped in the gravitational potential. The bound is saturated by non-rotating, uncharged BH's.

We remark that the existence of circular photon orbits and an instability timescale $\Delta t \approx 1/\lambda$ is a property common to many solutions in gravity, including BH-looking horizon-less geometries known as fuzzballs or BH microstate geometries with either flat or AdS asymptotics. A large class of horizon-free microstate geometries is known [13–15] (and references therein) including their stringy origin [16–19]. Geodesic motion in these geometries has been investigated in [20–24]. Here we focus on critical scattering for a class of three-charge BH microstate geometries with asymptotically flat or $AdS_3 \times S^3$ geometries. We find that only geodesics scattered in asymptotically flat micro-state geometries can reach the fuzzball photon-sphere, exhibiting random angular dispersion at infinity. More interestingly, we find that the Lyapunov exponent λ for a special class of asymptotically flat micro-state geometries is smaller than λ_b , which in turn is typically smaller than λ_H . Since λ is related to the time decay of QNM's dominating at late times the response of the geometry to perturbations, our results suggest that ring-down signals can be used to discriminate between BH's and geometries with non trivial micro-structures at the horizon scale⁶.

The plan of the paper is as follows. In Section 2 we discuss geodesics in asymptotically AdS Kerr-Newmann space-times in $d = 4$. We derive the Hamiltonian for massless probes and discuss radial and angular motion by stressing the role of the impact parameter(s). We then consider geodesics ending inside the horizon. In section 3 we study critical and nearly critical geodesics, we introduce the concepts of critical impact parameter b_c and Lyapunov exponent λ and propose a bound on the latter. In section 4 we discuss some BH examples in flat and AdS space-times. We also extend our analysis to arbitrary dimension d . In section 5 we discuss three-charge fuzzball micro-state geometries in the near horizon limit or, more interestingly, in flat space-time. Section 6 contains a discussion of our results and possible outlooks. In appendix we discuss integration of the angular motion in $d = 4$.

⁴The role of the ratio of λ , related to the minimum of the imaginary part of the quasi-normal mode frequency, and λ_H , related to the surface gravity of the inner horizon, based on [11] has been recently stressed in [12] in connection with the strong cosmic censorship. We thank J. Maldacena for pointing this out to us as well as the presence in this context of a sliver near extremality, similar to the one we find.

⁵We have an analytical proof of this bound only for spherically symmetric BH's and numerical evidences for rotating black holes in four dimensions.

⁶Similar proposals were recently put forward in different contexts for the modifications of gravity at the horizon scale [25, 26].

2 Geodesics on AdS Kerr-Newman space-times

2.1 The metric

We consider geodesic motion in asymptotically AdS_4 Kerr-Newmann space-time⁷ with metric [27]

$$ds^2 = -\frac{\Delta_r}{\rho^2} \left(dt - \frac{a \sin^2 \theta d\phi}{\alpha_\ell} \right)^2 + \frac{\Delta_\theta \sin^2 \theta}{\rho^2} \left(a dt - \frac{(a^2 + r^2) d\phi}{\alpha_\ell} \right)^2 + \frac{\rho^2 dr^2}{\Delta_r} + \frac{\rho^2 d\theta^2}{\Delta_\theta} \quad (2.1)$$

where

$$\begin{aligned} \Delta_r &= (a^2 + r^2) \left(\frac{r^2}{\ell^2} + 1 \right) - 2Mr + Q^2, & \rho^2 &= r^2 + a^2 \cos^2 \theta, \\ \Delta_\theta &= 1 - \frac{a^2}{\ell^2} \cos^2 \theta, & \alpha_\ell &= 1 - \frac{a^2}{\ell^2} \end{aligned} \quad (2.2)$$

with M the ‘mass’, $a = J/M$ the angular momentum ‘parameter’, ℓ the AdS radius and Q the charge. A BH exists for any choice of $a < \ell$ ⁸, Q and M such that Δ_r has at least a real positive root, and the horizon radius r_H is then the largest root.

A peculiar feature of the above metric is a non-zero angular velocity $\omega = g_{t\phi}/g_{tt}$ at infinity $\Omega_\infty = \omega|_\infty = -a/\ell^2$. The angular velocity that is relevant for the thermodynamics is the difference $\Omega = \Omega_H - \Omega_\infty$ with $\Omega_H = \omega|_{r_H} = a\alpha_\ell/(r_H^2 + a^2)$ the angular velocity at the horizon [27].

The Hawking temperature of the BH is given by

$$2\pi T = \frac{\Delta'_r(r_H)}{2(a^2 + r_H^2)} \quad (2.3)$$

If $\Delta'_r(r_H) = 0$, the BH is said to be extremal and the temperature vanishes. The explicit expression of r_H in terms of the BH parameters (M , a , Q and the AdS ‘radius’ ℓ) can be found using Cardano-Tartaglia formulae for the zeroes of a quartic polynomial. We will refrain from exposing it since it is quite cumbersome and not crucial for our analysis.

2.2 The Hamiltonian and momenta

In the Hamilton-Jacobi formulation of the geodesics equation, the Hamiltonian reads

$$\mathcal{H} = \frac{1}{2} g^{mn} P_m P_n$$

For a massless spin-less particle in the AdS Kerr-Newmann metric \mathcal{H} can be written in the ‘separate’ form

$$\mathcal{H} = \frac{1}{2\rho^2} \left(P_r^2 \Delta_r - \frac{(E(a^2 + r^2) - a\alpha_\ell P_\phi)^2}{\Delta_r} \right) + \frac{1}{2\rho^2} \left(P_\theta^2 \Delta_\theta + \frac{(aE \sin^2 \theta - \alpha_\ell P_\phi)^2}{\sin^2 \theta \Delta_\theta} \right) \quad (2.4)$$

⁷More precisely, the metric is not asymptotically AdS_4 but rather tends to a rotating Einstein universe with $\Omega_\infty = -a/\ell^2$.

⁸This guarantees the positivity of the $g_{\theta\theta}$ -component of the metric.

with $E = -P_t$ and P_ϕ conserved quantities. Following Carter, Teukolsky and Chandrasekhar [28], the null condition $\mathcal{H} = 0$ is solved by introducing a ‘separation’ constant K , representing the total angular momentum, and setting

$$K^2 = P_\theta^2 \Delta_\theta + \frac{(aE \sin^2 \theta - \alpha_\ell P_\phi)^2}{\sin^2 \theta \Delta_\theta} = -P_r^2 \Delta_r + \frac{(E(a^2 + r^2) - a\alpha_\ell P_\phi)^2}{\Delta_r} \quad (2.5)$$

Defining the impact parameters as

$$\zeta = \frac{P_\phi \alpha_\ell}{E} - a \quad , \quad b = \frac{K}{E} \quad (2.6)$$

equations (2.5) can be written in the form

$$\begin{aligned} \mathcal{R}(r) &= \frac{\Delta_r^2 P_r^2}{E^2} = (r^2 - a\zeta)^2 - b^2 \Delta_r \\ \Theta(\cos \theta) &= \frac{\Delta_\theta^2 P_\theta^2 \sin^2 \theta}{E^2} = b^2 \Delta_\theta \sin^2 \theta - (\zeta + a \cos^2 \theta)^2 \end{aligned} \quad (2.7)$$

with \mathcal{R} and Θ quartic polynomials of r and $\cos \theta$, respectively. While b (as well as a and E) can be taken to be non-negative without loss of generality, ζ can be negative or positive depending on P_ϕ . One can distinguish three classes of geodesics according to the sign of P_ϕ :

$$\begin{aligned} \zeta > -a & \quad \text{co-rotating} \\ \zeta = -a & \quad \text{non-rotating} \\ \zeta < -a & \quad \text{counter-rotating} \end{aligned} \quad (2.8)$$

We notice that at infinity

$$\mathcal{R}(r) \approx r^4 \left(1 - \frac{b^2}{\ell^2} \right) + O(r^2) \quad (2.9)$$

so positivity of P_r^2 requires⁹

$$b < \ell \quad (2.10)$$

In fact we will later see that b is also bounded from below for the motion to take place at all. Using the monotonically decreasing variable r as time variable in the branch where the geodesics evolves towards the BH, so that $\dot{r}, P_r < 0$, the equations of motion $\dot{x}^m = \partial \mathcal{H} / \partial P_m$ can be written in the form

$$\begin{aligned} \frac{dt}{dr} &= \frac{E}{\Delta_r P_r} \left[\frac{a(\zeta + a \cos^2 \theta)}{\Delta_\theta} + \frac{(r^2 + a^2)(r^2 - a\zeta)}{\Delta_r} \right] \\ \frac{d\phi}{dr} &= \frac{E \alpha_\ell}{\Delta_r P_r} \left[\frac{(\zeta + a \cos^2 \theta)}{\sin^2 \theta \Delta_\theta} + \frac{a(r^2 - a\zeta)}{\Delta_r} \right] \\ \frac{d\theta}{dr} &= \frac{\Delta_\theta P_\theta}{\Delta_r P_r} \end{aligned} \quad (2.11)$$

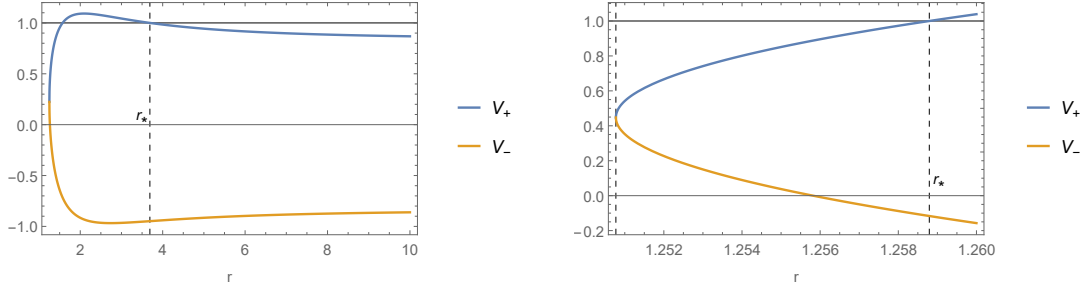


Figure 1: Effective potentials $V_{\pm}(r)$ for a BH with: $M = 1$, $\ell = 3$, $a = 0.7$, $Q = 0.3$ and impact parameters $\zeta = 0.5$ a) $b = 2.5$: The particle reaches the turning point r_* and returns to infinity b) $b = 8 > \ell$. Motion is allowed only inside a finite region of the space and geodesics always fall into the horizon.

2.3 Motion in the radial direction

We can view the motion in the radial direction as that of a particle in a one-dimensional potential. We write

$$\frac{\mathcal{R}(r)}{r^4} = [1 - V_+(r)][1 - V_-(r)] \quad (2.12)$$

with V_{\pm} the effective potentials

$$V_{\pm}(r) = \frac{a\zeta}{r^2} \pm \frac{b\sqrt{\Delta_r(r)}}{r^2} \quad (2.13)$$

Starting from infinity, a massless particle with large enough impact parameter b moves towards the BH till it reaches a turning point r_* , where $V_+(r_*) = 1$ and the radial velocity vanishes, see figure 1. After this point, the particle bounces back to infinity along a symmetrically reversed trajectory obtained by flipping the sign of the radial velocity.

Critical geodesics are obtained by tuning the impact parameters so that the value of $V_+(r)$ at the maximum is one, i.e.

$$V'_+(r_c) = 0 \quad \text{and} \quad V_+(r_c) = 1 \quad (2.14)$$

for some $r_c > r_H$. We will see that for b smaller than a critical value $b_c(\zeta_c)$, the potential satisfies $V_+(r) < 1$ for all $r > r_H$ and the geodesics finds no turning point. So, we can divide the impact parameter plane (b, ζ) into three regions

$$\begin{aligned} b < b_c(\zeta_c) & , & \text{absorption phase} \\ b_c(\zeta_c) < b < \ell & , & \text{scattering phase} \\ b > \ell & , & \text{only motion in the AdS interior} \end{aligned} \quad (2.15)$$

We will mainly focus on the second class of geodesics.

⁹One can also consider geodesics that never reach infinity and allow for $b > \ell$. We will comment on this case later on.

2.4 Motion in the θ direction

Motion along the θ direction takes place inside intervals bounded by the zeros of the quartic polynomial $\Theta(\cos\theta)$. Denoting $\chi = \cos\theta$, the polynomial Θ in (2.7) can be conveniently written in the form

$$\begin{aligned}\Theta(\chi) &= b^2 \left(1 - \frac{a^2\chi^2}{\ell^2}\right) (1 - \chi^2) - (\zeta + a\chi^2)^2 \\ &= A\chi^4 + B\chi^2 + C = A(\chi^2 - \chi_p^2)(\chi^2 - \chi_m^2)\end{aligned}\quad (2.16)$$

with

$$A = -a^2 \left(1 - \frac{b^2}{\ell^2}\right), \quad B = -b^2 \left(1 + \frac{a^2}{\ell^2}\right) - 2a\zeta, \quad C = b^2 - \zeta^2 \quad (2.17)$$

The zeros of the polynomial $\Theta(\chi)$ are located at

$$\chi_{p,m}^2 = \frac{-b^2 \left(1 + \frac{a^2}{\ell^2}\right) - 2a\zeta \mp \sqrt{\Delta}}{2a^2 \left(1 - \frac{b^2}{\ell^2}\right)} \quad (2.18)$$

with

$$\Delta = b^2 \left[b^2 \left(1 + \frac{a^2}{\ell^2}\right)^2 + 4a^2 \left(1 + \frac{\zeta^2}{\ell^2}\right) + 4a\zeta \left(1 + \frac{a^2}{\ell^2}\right) \right]. \quad (2.19)$$

Geodesic motion is allowed for choices of the parameters (b, ζ) such that $P_\theta^2 > 0$ for some $\chi \in [-1, 1]$. To determine this region it is convenient to write P_θ in the following form

$$\frac{P_\theta^2 \Delta_\theta}{E^2} = b^2 - V_{\text{eff}}(\chi) \quad (2.20)$$

with the angular effective potential

$$V_{\text{eff}}(\chi) = \frac{(\zeta + a\chi^2)^2}{\left(1 - \frac{a^2\chi^2}{\ell^2}\right)(1 - \chi^2)} \quad (2.21)$$

The effective potential is even in χ and bounded from below inside the interval $[-1, 1]$. For $\zeta = -a$ it has a maximum at $\chi_* = 0$, and minima at $\chi_* = \pm 1$. For $\zeta \neq -a$ it reaches infinity at $\chi = \pm 1$. The extrema of the potential (solutions of $V'_{\text{eff}}(\chi_*) = 0$) are located at $\chi = \pm\chi_*$ (if real and with $\chi_*^2 \leq 1$) with

$$\chi_*^2 = \left\{ 0, -\frac{\zeta}{a}, \frac{\ell^2(\zeta - \zeta_*)}{a(\ell^2 - \zeta\zeta_*)} \right\} \quad \text{with} \quad \zeta_* = -\frac{2a\ell^2}{\ell^2 + a^2} \quad (2.22)$$

and

$$V_{\text{eff}}(\chi_*) = \left\{ \zeta^2, 0, -\frac{4a\ell^2(\zeta + a)(\ell^2 + a\zeta)}{(\ell^2 - a^2)^2} \right\} \quad (2.23)$$

We are interested on geodesics starting from infinity, so we will take $b^2 < \ell^2$. In addition b^2 should be bigger than the absolute minimum of $V_{\text{eff}}(\chi_*)$ inside the interval $\chi \in [-1, 1]$. Depending on the value of ζ , the profile of $V_{\text{eff}}(\chi)$ changes and the global minimum can be located at any of the three extrema in (2.22). We have two different allowed regions:

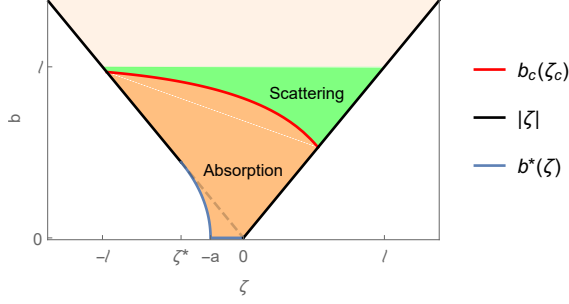


Figure 2: Allowed regions (green, red and light red) in the ζ, b plane of a BH with parameters: $M = 1$, $\ell = 3$, $a = 0.7$. Geodesics in the light red region does not reach infinity.

A) The geodesics bounces inside the interval $\chi \in [-\chi_p, \chi_p]$ for

$$-\ell < \zeta < \ell \quad \text{and} \quad |\zeta| < b < \ell \quad (2.24)$$

For $\zeta_* < \zeta < 0$, the effective potential has two minima and a maximum in $\chi = 0$, while outside this interval the potential has a unique minimum in $\chi = 0$.

B) The geodesics bounces inside the interval $\chi \in [-\chi_p, -\chi_m]$ or $\chi \in [\chi_m, -\chi_m]$

$$\zeta_* < \zeta < 0 \quad \text{and} \quad b_*(\zeta) < b < |\zeta| \quad (2.25)$$

with

$$b_*^2(\zeta) = \begin{cases} -\frac{4a\ell^2(\zeta+a)(\ell^2+a\zeta)}{(\ell^2-a^2)^2} & \text{for } \zeta_* < \zeta < -a \\ 0 & \text{for } -a < \zeta < 0 \end{cases} \quad (2.26)$$

The effective potential has two minima and a maximum in $\chi = 0$.

We display in colors the allowed region in the impact parameter plane (b, ζ) in figure 2. Geodesics belonging to the classes A and B correspond to the regions above and below $b = |\zeta|$ (dashed line in the graph) respectively. We distinguish with two colors, red and green, the absorption and scattering phases respectively (see below for details). The light red region collects all geodesics allowed by the kinematics that cannot reach the AdS boundary at infinity. Geodesics in this class always fall into the horizon.

In figure 3, we display the form of $V_{\text{eff}}(\chi)$ for various choices of ζ setting $a = 1$, $\ell = 2$, $Q = 0.3$. Geodesic motion is allowed when $V_{\text{eff}}(\chi)$ is below the b^2 -dashed line and it bounces inside the intervals limited by the intersection points of the two graphs. Whenever b^2 coincides with an extremum of $V_{\text{eff}}(\chi)$ one has either a shear-free (un)stable geodesics at fixed $\theta = \theta_0$ or a critical geodesics at the equator (see next section). Geodesics at fixed θ -angle are stable around the minima of $V_{\text{eff}}(\chi)$, and unstable around the maximum.

We will see in the next section that critical geodesics always correspond to the case $b > |\zeta|$, so critical motion will always bounce inside the interval $\chi \in [-\chi_+, \chi_+]$ with $\chi_+ = 1$ for $\zeta = -a$.

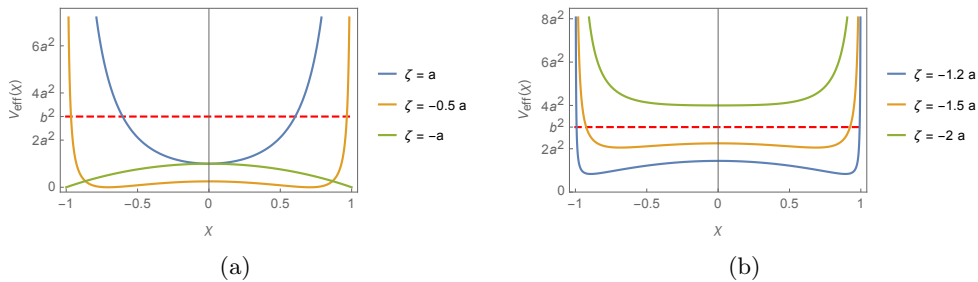


Figure 3: Effective potential $V_{\text{eff}}(\chi)$ for a BH with angular parameter $a = 0.7$, $\ell = 3$: (a) Co-rotating and non-rotating geodesics (b) Counter-rotating geodesics.

2.5 Geodesics inside the absorption region

For $b < b_c(\zeta_c)$, the particle falls inside the BH horizon. It is important to observe that near the horizon both radial and angular velocities along the ϕ -direction are independent of the impact parameters (b, ζ) . Indeed expanding (2.11) near $r \approx r_H$ one finds $\mathcal{R} \approx (r_H^2 - a\zeta)^2$ leading to

$$\frac{dr}{dt} \approx \frac{\Delta'_r(r_H)(r - r_H)}{(a^2 + r_H^2)} \quad , \quad \frac{dr}{d\phi} \approx \frac{\Delta'_r(r_H)(r - r_H)}{\alpha_\ell a} \quad , \quad \frac{dr}{d\chi} \approx -\frac{(r_H^2 - a\zeta)}{\sqrt{\Theta(\chi)}} \quad (2.27)$$

We notice that near the horizon both the distance from the horizon and the radial velocity vanish but their ratio

$$\lambda_H = -\frac{1}{2(r - r_H)} \frac{dr}{dt} \Big|_{r_H} \approx \frac{\Delta'_r(r_H)}{2(a^2 + r_H^2)} = 2\pi T \quad (2.28)$$

is finite and proportional to the BH temperature. We will show later that λ_H is typically bigger than the ratio λ describing the vanishing rate of the radial velocity at the photon-sphere. This inequality is however violated for extremal and near-extremal black holes.

Shear free geodesics

A particular simple class of geodesics in the absorption phase are the so called shear-free geodesics (radial falling) corresponding to trajectories with zero total angular momentum. For $b = 0$, non-negativity of P_θ^2 requires that the polynomial $\Theta(\cos\theta)$ in (2.7) exactly vanishes. This happens when the impact parameter ζ and the initial angle θ_0 are related by

$$\zeta = -a \cos^2 \theta_0 \quad (2.29)$$

For this choice $\dot{\theta} = 0$, i.e. $\theta = \theta_0$ along the whole trajectory. Plugging these values into the polynomial $\mathcal{R}(r)$ one finds

$$\mathcal{R}(r) = (r^2 + a^2 \cos^2 \theta_0)^2 \quad (2.30)$$

that is strictly positive, so no turning points are found before the geodesics reaches the BH horizon. The rates of change of t , ϕ and θ with r take the simple form

$$\frac{dt}{dr} = \frac{a^2 + r^2}{\Delta_r(r)} \quad , \quad \frac{d\phi}{dr} = \frac{\alpha_\ell a}{\Delta_r(r)} \quad , \quad \frac{d\theta}{dr} = 0 \quad (2.31)$$

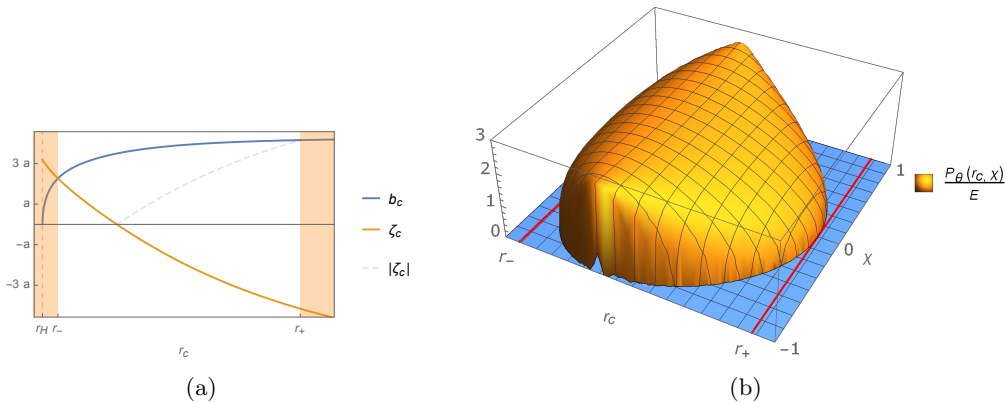


Figure 4: (a) Plots of $b_c(r_c)$ and $\zeta_c(r_c)$. (b) Plot of $P_\theta(r_c, \chi)$ for AdS Kerr-Newman BH's with mass $M = 1$, AdS radius $\ell = 3$, angular momentum $a = 0.7$ and charge $Q = 0.3$.

that reduce to (2.27) near the horizon.

3 Critical and nearly critical geodesics

In this section we study critical and nearly critical geodesics in asymptotically AdS Kerr-Newman BH's.

3.1 Critical geodesics

A critical geodesics is obtained when the two largest roots of the polynomial

$$\mathcal{R}(r) = (r^2 - a\zeta)^2 - b^2 \Delta_r \quad (3.1)$$

coincide. More precisely, we say that a geodesics is critical, if the largest zero r_c of $\mathcal{R}(r)$ is a double zero, or in other words

$$\mathcal{R}(r_c) = \mathcal{R}'(r_c) = 0 \quad (3.2)$$

These equations can be easily solved for ζ and b as a function of the critical radius

$$b_c(r_c) = \frac{4r_c \sqrt{\Delta_r(r_c)}}{\Delta_r'(r_c)} \quad , \quad \zeta_c(r_c) = \frac{r_c^2}{a} - \frac{4r_c \Delta_r(r_c)}{a \Delta_r'(r_c)} \quad (3.3)$$

Plugging these formulae into $\Theta(\chi)$, one finds that the polynomial is positive for r_c belonging to a finite interval

$$r_c \in [r_-, r_+] \quad (3.4)$$

wherein

$$b_c(r_c)^2 \geq \zeta_c(r_c)^2 \quad (3.5)$$

with r_\pm saturating the inequality. We remark that for non-extremal BH's , r_- is always outside the horizon since equations (3.2) do not admit any solution with $r_c = r_H$ unless

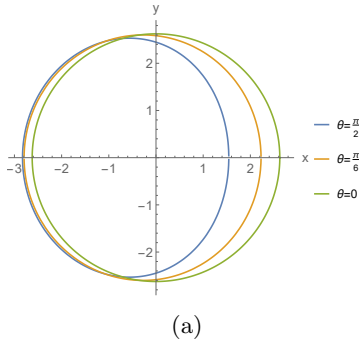


Figure 5: (a) Shadow of a BH in AdS space with parameters $\ell = 3$, $M = 1$, $a = 0.7$, $Q = 0.3$ as seen by an observer with inclination $\theta = 0$, $\theta = \pi/6$ and $\theta = \pi/2$ (equatorial plane).

$\Delta'(r_H) = 0$. On the other hand, one can see that depending on the masses, angular momentum and charges, r_- can be either inside or outside the ergo-region.

Geodesics saturating the inequality in (3.5) lie on the equatorial plane $\chi = \dot{\chi} = 0$ and their impact parameters take the simple form

$$b_{\pm} = \mp \zeta_{\pm} = \frac{4 r_{\pm} \sqrt{\Delta_r(r_{\pm})}}{\Delta'_r(r_{\pm})} \quad (3.6)$$

where $\zeta_{\pm} = \zeta(r_{\pm})$ and $b_{\pm} = b_c(r_{\pm})$.

On the other hand, critical geodesics with r_c inside the interval $[r_-, r_+]$ display a non-trivial motion in the θ direction. In figure 4 we display the dependence of (ζ_c, b_c) and P_{θ} on the critical radius r_c . We notice that in the region where P_{θ}^2 is positive and therefore motion is allowed $b_c > |\zeta_c|$, so critical geodesics fall always into the first of the two classes identified in Section 2.3. The motion in the χ -plane is confined inside the interval $[-\chi_+, \chi_+]$.

The collection of all points leading to a critical geodesics delimits the edge of the BH shadow as seen by an observer at infinity. For an observer on a plane at fixed θ , the rim of the shadow is defined by the parametric curve [28]

$$(x - x_0)^2 + y^2 = b_c^2 \quad (3.7)$$

where

$$y = \frac{P_{\theta}(r_c) \sqrt{\Delta_{\theta}}}{E}, \quad x = \frac{\alpha_{\ell} P_{\phi}(r_c)}{E \sin \theta \sqrt{\Delta_{\theta}}}, \quad x_0 = \frac{a \sin \theta}{\sqrt{\Delta_{\theta}}} \quad (3.8)$$

with r_c running inside the sub-interval of (3.4) allowed by the chosen value of $\chi = \cos \theta$, see Fig. 4. In figure 5 we depict the shadow of a Kerr-Newmann AdS BH for particular values of mass M , charge Q and angular momentum parameter a at different values of $\theta = 0, \pi/6, \pi/2$. Note the asymmetric shape, due to the rotation, as one approaches the equatorial plane $\theta = \pi/2$.

3.2 The Lyapunov exponent

In this section we consider nearly critical geodesics along the equatorial plane ($\theta = \pi/2$, $\chi = 0$) and compute the Lyapunov exponent determining the exponential growth with time of geodesic deviation.

Approaching the critical radius $r \approx r_c$ with $\chi = \dot{\chi} = 0$, the radial velocity (2.11) vanishes as

$$\frac{dr}{dt} \approx -2\lambda(r - r_c) \quad (3.9)$$

with

$$\lambda = \frac{1}{2} \sqrt{\frac{\mathcal{R}''(r_c)}{2}} \frac{\Delta_r(r_c)}{a\zeta_c \Delta_r(r_c) + (r_c^2 - a\zeta_c)(a^2 + r_c^2)} \quad (3.10)$$

and

$$\mathcal{R}''(r_c) = 12r_c^2 - 4a\zeta_c - b_c^2 \Delta_r''(r_c) \quad (3.11)$$

We will now show that λ , governing the vanishing rate of \dot{r} , coincides with the Lyapunov exponent of nearly critical geodesics scattered around $r \approx r_c$. A nearly critical geodesics can be obtained by varying the impact parameters (b, ζ) slightly away from the critical values (b_c, ζ_c) . There are two distinct cases depending on whether the variation lifts the double zero or splits it into two. In the former case, the turning point disappears and the (massless) particle falls into the BH. We are interested in the latter case whereby the (massless) particle reaches the largest of the two nearby zeroes and bounces back to infinity. Near the critical point the polynomial $\mathcal{R}(r)$ can be approximated by

$$\mathcal{R}(r) \approx c[(r - r_c)^2 - \epsilon^2] = c(r - r_c - \epsilon)(r - r_c + \epsilon) \quad (3.12)$$

where ϵ parametrises the distance between the critical radius and the turning point of the nearly critical geodesics located at $r_* = r_c + \epsilon$. The time delay to reach r_* and get back becomes

$$\Delta t = 2 \int^{r_*} \frac{dr}{\dot{r}} \approx -\frac{1}{\lambda} \int^{r_*} \frac{dr}{\sqrt{(r - r_*)(r - r_c + \epsilon)}} \approx -\frac{1}{\lambda} \log \epsilon \quad (3.13)$$

where (3.9) has been used. Similarly for the deflection angle one finds

$$\Delta\phi = 2 \int^{r_*} \frac{\dot{\phi} dr}{\dot{r}} \approx -\frac{\omega_c}{\lambda} \int^{r_*} \frac{dr}{\sqrt{(r - r_*)(r - r_c + \epsilon)}} \approx -\frac{\omega_c}{\lambda} \log \epsilon \quad (3.14)$$

with

$$\omega_c = \dot{\phi}(r_c) = \alpha_\ell \left[\frac{\zeta_c \Delta_r(r_c) + a(r_c^2 - a\zeta_c)}{a\zeta_c \Delta_r(r_c) + (r_c^2 + a^2)(r_c^2 - a\zeta_c)} \right] \quad (3.15)$$

the angular velocity at the critical point. Taking the variation with respect to the deviation in the incoming momenta one finds

$$\frac{\delta(\Delta\phi)}{\delta P_\phi} \sim \frac{\delta(\Delta\phi)}{\delta\epsilon} \approx \frac{\omega_c}{\lambda\epsilon} \approx \frac{\omega_c}{\lambda} e^{\lambda\Delta t} \quad (3.16)$$

We conclude that the Lyapunov exponent λ is determined by the vanishing rate (3.9) of the radial velocity of an infalling neutral massless particle at the photon-sphere.

In figures 6 we plot the functions (3.10) $\lambda_\pm = \lambda(r_\pm)$, the minimum and maximum values of λ , λ_H and

$$\lambda_b = \frac{1}{2b_{\min}} \quad (3.17)$$

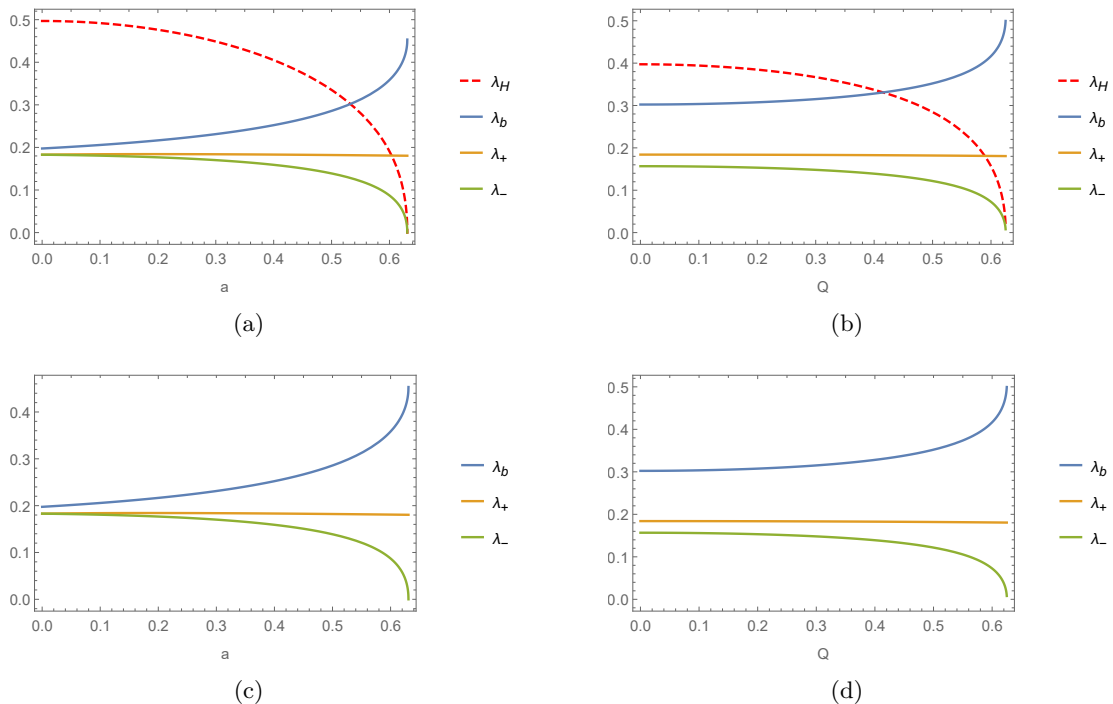


Figure 6: (a,b) Comparison between the Lyapunov exponents of a BH with $M = 1$, $\ell = 3$ and its temperature as a function of the rotation parameter a (left, $Q = 0.7$) and the BH charge Q (right $a = 0.7$). (c,d) The BH temperature has been removed to highlight the hierarchy between λ_b , λ_+ and λ_- .

as functions of the angular momentum and charge, where $b_{\min} = b_c(r_-)$ is the minimal choice of the impact parameter that an impinging massless particle can have without falling into the BH's. We notice that $\lambda \leq \lambda_b$ with the bound saturated for non-rotating and uncharged BH's.

4 Analytic results for specific BH's

In this section we compute the Lyapunov exponents and critical impact parameters for some simple instances of BH's in $d = 4$ and then present some general results for non-rotating BH's in arbitrary dimensions. For simplicity we focus on geodesics with $\dot{\chi} = 0$, corresponding to one of the choices $r_c = r_{\pm}$. In all the examples we compare the results for λ with the one for λ_H characterising the vanishing rate of the radial velocity at the horizon and given by

$$\lambda_H = 2\pi T = \frac{\Delta'_r(r_H)}{2(a^2 + r_H^2)} \quad (4.1)$$

4.1 Non rotating BH's in AdS

We consider first the case of a non-rotating charged BH in AdS, i.e. $a = 0$. The metric reads

$$ds^2 = -\frac{\Delta_r}{r^2} dt^2 + r^2 \sin^2 \theta d\phi^2 + \frac{r^2 dr^2}{\Delta_r} + r^2 d\theta^2 \quad (4.2)$$

with

$$\Delta_r(r) = \frac{r^4}{\ell^2} + r^2 - 2Mr + Q^2, \quad (4.3)$$

The peculiar feature of the non-rotating case, is that due to full rotational symmetry, the radial velocity of a probe depends only on the total angular momentum $K = bE$, so the critical equations determine both b and the critical radius r_c , leaving ζ undetermined. The photon-sphere is a round sphere with critical radius given in terms of the BH mass and charge. The critical equations reduce to

$$r_c^4 - b_c^2 \Delta_r(r_c) = 4 \Delta_r(r_c) - r_c \Delta_r'(r_c) = 0 \quad (4.4)$$

that can be solved for r_c and b_c .

Schwarzschild BH in flat space-time

Setting $Q = 0$ and sending $\ell \rightarrow \infty$, one gets a Schwarzschild BH in flat space-time for which

$$r_c = 3M \quad , \quad b_c = 3\sqrt{3}M \quad , \quad \lambda = \frac{1}{2b_c} \quad (4.5)$$

We notice that

$$\lambda = \lambda_b = \frac{1}{2b_c} = \frac{1}{6\sqrt{3}M} < \lambda_H = \frac{1}{4M} \quad (4.6)$$

Reissner-Norsdtröm BH in flat space-time

Sending $\ell \rightarrow \infty$ with $Q \neq 0$ one finds

$$b_c = \sqrt{\frac{2r_c^3}{r_c - M}} \quad , \quad \lambda = \frac{1}{2b_c} \sqrt{2 - \frac{3M}{r_c}} \quad (4.7)$$

with

$$r_c = \frac{1}{2} \left(3M + \sqrt{9M^2 - 8Q^2} \right) \quad , \quad (4.8)$$

and $0 < Q \leq M$. We notice that $\lambda < \lambda_b$ in the charged case. Comparing with

$$\lambda_H = \frac{r_H - M}{r_H^2} \quad (4.9)$$

one finds that the bound $\lambda < \lambda_H$ is violated inside the very narrow window $0.99M < Q \leq M$ near extremality, where $\lambda > \lambda_H$. In particular, in the extremal case $Q = M$, $\lambda_H = 0$, while for $\lambda = \lambda_{\text{ext}}$ one finds

$$r_c = 2M \quad , \quad b_c = 4M \quad , \quad \lambda_{\text{ext}} = \frac{1}{8\sqrt{2}M} > \lambda_H = 0 \quad (4.10)$$

AdS-Schwarzschild BH

Setting $Q = 0$ with ℓ finite, one finds

$$r_c = 3M \quad , \quad b_c = \frac{3\sqrt{3}M\ell}{\sqrt{27M^2 + \ell^2}} \quad , \quad \lambda = \frac{1}{2b_c} \quad (4.11)$$

Solving $\Delta_r(r_H) = 0$ for M in favor of r_H , it is easy to check that $\lambda < \lambda_H$ for any r_H and ℓ .

AdS-Reissner-Norsdtröm BH

Keeping $Q \neq 0$ one finds

$$b_c = \sqrt{\frac{2\ell^2 r_c^3}{2r_c^3 + \ell^2(r_c - M)}} \quad , \quad \lambda = \frac{1}{2b_c} \sqrt{2 - \frac{3M}{r_c}} \quad (4.12)$$

with

$$r_c = \frac{1}{2} \left(3M + \sqrt{9M^2 - 8Q^2} \right) \quad (4.13)$$

Note that $2M \leq r_c \leq 3M$, so

$$\lambda \leq \lambda_b = \frac{1}{2b_c} \quad (4.14)$$

with the bound saturated for $Q = 0$.

4.2 Rotating BH's

Expressions for λ in the general case of rotating BH's are quite involved so we limit ourselves to special choices of the parameters such that analytic formulae can be found.

Large photon-spheres

In the limit where the size ℓ of Anti-deSitter is much smaller than the radius of the photon-sphere, i.e. $a, \ell \ll M, Q, r_c$ one finds

$$b_{\pm} = \mp \zeta_{\pm} \approx \ell \quad , \quad r_{\pm} \approx \frac{3M + \sqrt{9M^2 - 8Q^2} (1 \mp \frac{a}{\ell})^2}{2(1 \mp \frac{a}{\ell})^2} \quad (4.15)$$

For the Lyapunov exponents one finds

$$\lambda_{\pm} \approx \frac{\sqrt{3M r_{\pm} - 4Q^2}}{2\ell r_{\pm} (1 \mp \frac{a}{\ell})} < \frac{\sqrt{3M r_{\pm} - 2Q^2}}{2\ell r_{\pm} (1 \mp \frac{a}{\ell})} = \frac{1}{2\ell} = \lambda_b \quad (4.16)$$

as expected.

Extremal asymptotically flat Kerr-Newman BH

The extremal Kerr-Newman BH in flat space-time ($\ell = \infty$) is obtained by taking

$$M = r_H \quad , \quad Q^2 = r_H^2 - a^2 \quad (4.17)$$

leading to

$$\Delta_r = (r - r_H)^2 \quad (4.18)$$

One finds

$$\begin{aligned} r_- &= 2(r_H - a) \quad , \quad b_- = \zeta_- = 2(r_H - a) \\ r_+ &= 2(r_H + a) \quad , \quad b_+ = -\zeta_+ = 2(r_H + a) \end{aligned} \quad (4.19)$$

Here we assume that $a < r_H/2$, in order to ensure that r_- is outside the BH horizon. For the Lyapunov exponents one finds

$$\lambda_{\pm} = \frac{1}{2(4r_H - 3a)} \left(\frac{r_H - 2a}{2r_H - 2a} \right)^{\frac{3}{2}} \quad (4.20)$$

We notice that $\lambda > \lambda_H = 0$, so the bound is violated as claimed.

4.3 Spherical symmetric BH's in higher dimensions

We now extend our analysis and consider critical null geodesics around spherically symmetric BH's in d -dimensions with AdS or flat asymptotics. The line element of an asymptotically AdS_d spherically symmetric BH reads

$$ds^2 = -f(r)dt^2 + f(r)^{-1}dr^2 + r^2 ds_{S^{d-2}}^2 \quad (4.21)$$

where

$$f(r) = 1 - \frac{2M}{r^{d-3}} + \frac{Q^2}{r^{2(d-3)}} + \frac{r^2}{\ell^2} \quad (4.22)$$

and M, Q, ℓ describing the mass, charges and AdS radius of the asymptotic geometry. The Hamiltonian null condition reads

$$\mathcal{H} = f(r) P_r(r)^2 - \frac{E^2}{f(r)} + \frac{K^2}{r^2} = 0 \quad (4.23)$$

with K denoting the total angular momentum. The radial velocity reads

$$\frac{dr}{dt} = \frac{f(r)^2 P_r}{E} = \frac{f(r)}{r} \sqrt{\mathcal{R}(r)} \quad (4.24)$$

with $b = K/E$ the impact parameter and

$$\mathcal{R}(r) = r^2 - b^2 f(r) \quad (4.25)$$

Near the horizon one finds the radial velocity vanishing as

$$\frac{dr}{dt} \approx -2\lambda_H(r - r_H) \quad (4.26)$$

with

$$\lambda_H = \frac{f'(r_H)}{2r_H} \sqrt{\mathcal{R}(r_H)} = \frac{f'(r_H)}{2} = 2\pi T \quad (4.27)$$

given in terms of the BH temperature T . The BH photon-sphere is defined by the critical equations $\mathcal{R}(r_c) = \mathcal{R}'(r_c) = 0$ leading to

$$b_c^2 = \frac{r_c^2}{f(r_c)} \quad (4.28)$$

with r_c solving

$$r_c f'(r_c) = 2f(r_c) \quad (4.29)$$

Near the critical radius one finds

$$\frac{dr}{dt} \approx -2\lambda(r - r_c) \quad (4.30)$$

with

$$\lambda = \frac{f(r_c)}{2r_c} \sqrt{\frac{\mathcal{R}''(r_c)}{2}} = \frac{\sqrt{d-3}}{2b_c} \sqrt{1 - (d-2) \frac{Q^2}{r_c^{2(d-3)}}} \quad (4.31)$$

Note that λ is bounded from above

$$\lambda \leq \lambda_b = \frac{\sqrt{d-3}}{2b_c} \quad (4.32)$$

with the bound saturated by the uncharged BH's. For $Q = 0$ one finds

$$\lambda = \frac{\sqrt{d-3}}{2b_c} \quad (4.33)$$

with

$$b_c = \frac{r_c}{\sqrt{f(r_c)}} \quad , \quad r_c^{d-3} = 2M \left(\frac{d-1}{2} \right) \quad (4.34)$$

Quite remarkably r_c does not depend on ℓ but b_c does.

5 Fuzzball geometries

In this section we study critical and nearly critical null geodesics in a class of three-charge microstate geometries of type $(1, 0, n)$ first introduced in [15, 29]. We consider both the asymptotically flat and the near-horizon limit exhibiting pretty different behaviour. We focus on scattering along the $\vartheta = 0$ direction, where the geodesic equations have been shown to be integrable in this class of microstate geometries. We will also set $Q_1 = Q_5 = L^2$ for notational simplicity. The geometries are characterized by an asymptotically $AdS_3 \times S^3$ metric that after a conformal rescaling¹⁰ can be written as

$$ds_6^2 = -2(dv + \beta)(du + \gamma) + Z^2 ds_4^2. \quad (5.1)$$

with

$$ds_4^2 = (\rho^2 + a^2 \cos^2 \vartheta) \left(\frac{d\rho^2}{\rho^2 + a^2} + d\vartheta^2 \right) + (\rho^2 + a^2) \sin^2 \vartheta d\varphi^2 + \rho^2 \cos^2 \vartheta d\psi^2. \quad (5.2)$$

the flat space metric on \mathbb{R}^4 in oblate spheroidal coordinates. For $\vartheta = 0$, the various functions entering in the metric take the form

$$Z = 1 + \frac{L^2}{\rho^2 + a^2} \quad , \quad \beta = -\frac{a^2 R}{\rho^2 + a^2} d\psi \quad , \quad \gamma = \frac{a^2 R (1 - \mathcal{F}_n)}{\rho^2 + a^2} d\psi + \mathcal{F}_n dv \quad (5.3)$$

and¹¹

$$\mathcal{F}_n(\rho) = (1 - \nu) \left[1 - \left(\frac{\rho^2}{\rho^2 + a^2} \right)^n \right] \quad , \quad \nu \equiv \frac{L^4}{2a^2 R^2} \quad (5.4)$$

¹⁰We recall that conformal rescalings are irrelevant for the study of null geodesics.

¹¹In the notation of [23] $\epsilon_1 = \epsilon_4^2 = 2a^2(\nu - 1)$.

Motion along the $\vartheta = 0$ direction requires $P_{\vartheta} = P_{\varphi} = 0$, so the Hamiltonian reduces to

$$\mathcal{H} = \frac{P_{\rho}^2}{2Z^2} - P_u(P_v - \mathcal{F}_n P_u) + \frac{[P_{\psi}(\rho^2 + a^2) + a^2 R(P_v - P_u)]^2}{2Z^2 \rho^2 (\rho^2 + a^2)^2} \quad (5.5)$$

We set

$$P_u = \frac{E + P_y}{\sqrt{2}} \quad , \quad P_v = \frac{E - P_y}{\sqrt{2}} \quad (5.6)$$

and focus on the case $P_y = 0$. For this choice the Hamiltonian reduces to

$$\mathcal{H} = \frac{\rho^2 P_{\rho}^2 + P_{\psi}^2}{2Z^2 \rho^2} - \frac{E^2}{2}(1 - \mathcal{F}_n) \quad (5.7)$$

and the velocities w.r.t. the radial variable are given by

$$\frac{dt}{d\rho} = -\frac{\partial \mathcal{H} / \partial E}{\partial \mathcal{H} / \partial P_{\rho}} = \frac{Z(\rho)^2 E [1 - \mathcal{F}_n(\rho)]}{P_{\rho}(\rho)} \quad , \quad \frac{d\psi}{d\rho} = \frac{\partial \mathcal{H} / \partial P_{\psi}}{\partial \mathcal{H} / \partial P_{\rho}} = -\frac{P_{\psi}}{P_{\rho}(\rho) \rho^2} \quad (5.8)$$

with

$$\frac{P_{\rho}(\rho)}{E} = \sqrt{\mathcal{R}(\rho)} = \sqrt{Z(\rho)^2 [1 - \mathcal{F}_n(\rho)] - \frac{b^2}{\rho^2}} \quad (5.9)$$

and $b = P_{\psi}/E$. We notice that positivity of $\mathcal{R}(\rho)$ at infinity requires

$$b^2 < 2L^2 \quad (5.10)$$

The critical equations

$$\mathcal{R}(\rho_c) = \mathcal{R}'(\rho_c) = 0 \quad (5.11)$$

can be solved for b_c and ρ_c . Near the critical radius one finds

$$\frac{d\rho}{dt} \approx -2\lambda(\rho - \rho_c) \quad (5.12)$$

with

$$\lambda = \frac{\sqrt{\mathcal{R}''(\rho_c)/2}}{2Z^2(\rho_c)(1 - \mathcal{F}_n(\rho_c))} \quad (5.13)$$

5.1 The BH geometry

The BH geometry corresponding to the above micro-states is obtained by sending $a \rightarrow 0$, $\nu \rightarrow \infty$ and $n \rightarrow 0$ keeping finite the product

$$L_p^2 = n \nu a^2 \quad (5.14)$$

leading to

$$\mathcal{F}_n = -\frac{L_p^2}{\rho^2} \quad , \quad Z = 1 + \frac{L^2}{\rho^2} \quad (5.15)$$

The radial function $\mathcal{R}(\rho)$ becomes

$$\mathcal{R}(\rho) = 1 + \frac{3L^2 - b^2}{\rho^2} + \frac{3L^4}{\rho^4} + \frac{L^6}{\rho^6} \quad (5.16)$$

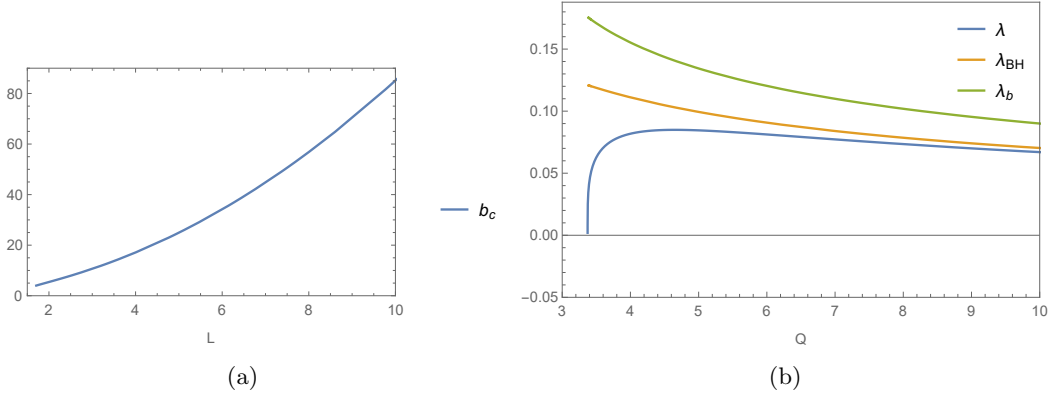


Figure 7: Critical impact parameter b_c (a) and Lyapunov exponent (b) as a function of the fuzzball charge L , for $a = 1$, and $n = 1$.

The critical radius and impact parameters read

$$\rho_c = \sqrt{2} L \quad , \quad b_c = \frac{3\sqrt{3}}{2} L \quad (5.17)$$

leading to the Lyapunov exponent

$$\lambda_{BH} = \frac{2}{9L} \quad (5.18)$$

We notice (fig. 7) that $\lambda_{BH} < 1/(\sqrt{2}b_c)$. The asymptotically AdS solution can be analysed by simply dropping the 1 in Z . It is easy to see that no solutions to the critical equations are found in this case.

5.2 The asymptotically flat fuzzball

In the case of the asymptotically flat fuzzball the critical equations can be written in the form

$$\begin{aligned} b_c(\rho_c) &= \rho_c Z(\rho_c) \sqrt{1 - \mathcal{F}_n(\rho_c, \nu)} \\ 2[1 - \mathcal{F}_n(\rho_c, \nu)] (\rho_c Z'(\rho_c) + Z(\rho_c)) - Z(\rho_c) \rho \mathcal{F}'_n(\rho_c, \nu) &= 0 \end{aligned} \quad (5.19)$$

The second equation is linear in ν and can be solved for $\nu = \nu(\rho_c)$ that then can be plugged into the first equation to determine $b_c(\rho_c)$. For instance for $n = 1$ one finds

$$\begin{aligned} b_c(\rho_c) &= \frac{\rho_c^2}{(\rho_c^2 + a^2)} \sqrt{\frac{(\rho_c^2 + a^2 + L^2)^3}{\rho_c^2(2L^2 - a^2) - a^4 - a^2L^2}} \\ \nu(\rho_c) &= \frac{\rho_c^2[\rho_c^4 + \rho_c^2(3a^2 - L^2) + 2a^4 + 2a^2L^2]}{a^2[\rho_c^2(2L^2 - a^2) - a^4 - a^2L^2]} \end{aligned} \quad (5.20)$$

Near the critical radius one finds

$$\frac{d\rho}{dt} \approx -2\lambda(\rho - \rho_c) \quad (5.21)$$

with

$$\lambda = \frac{\sqrt{\mathcal{R}''(\rho_c)/2}}{2Z^2(\rho_c)(1 - \mathcal{F}_n(\rho_c))} \quad (5.22)$$

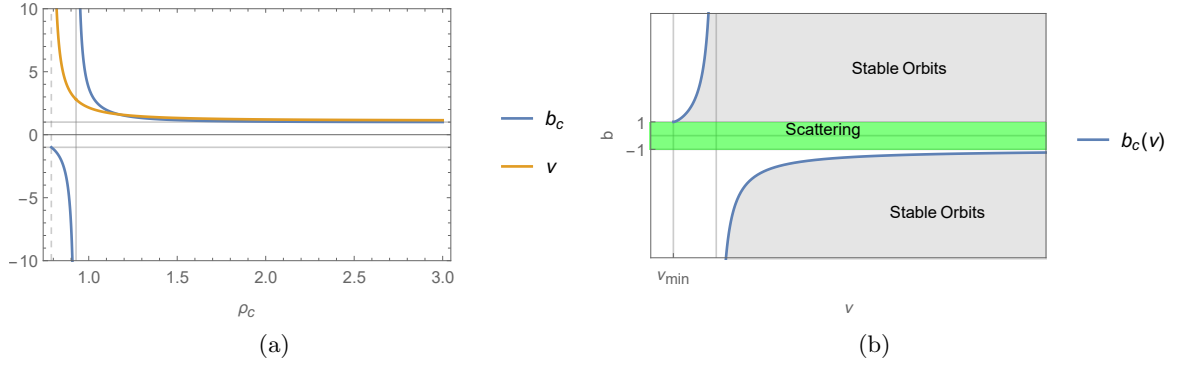


Figure 8: (a) Critical impact parameter b_c and geometric parameter ν allowing for circular photon orbits as a function of the critical radius ρ_c , a is set to 1. (b) Parameter space for null geodesics with zero total angular momentum.

The functions $b_c(\rho_c)$, $\nu(\rho_c)$, $\lambda(\rho_c)$ can be used to plot parametrically $b_c(\nu)$, $\lambda(\nu)$. The plots are displayed in figure 8 for a fuzzball solution with $n = 1$ and $L = 5$. Plot 7 shows that λ is below the bound (in $d = 5$)

$$\lambda < \lambda_b = \frac{1}{\sqrt{2b_c}} \quad (5.23)$$

We notice also that λ of the fuzzball is smaller than the Lyapunov exponent λ_{BH} (5.18) associated to the BH of the same charge.

5.3 Asymptotically AdS geometry

The asymptotically AdS case is obtained by dropping the 1 term in Z .¹² The positivity of P_ρ^2 at infinity requires $P_\psi = 0$ so only geodesics moving entirely inside AdS_3 can arrive from the AdS boundary¹³.

Starting from infinity, geodesics evolve until they reach the turning point ρ_* , i.e. a zero of $P_\rho(\rho)$, where the radial velocity vanishes. Zeros of $P_\rho(\rho)$ coincide with the ones of the function

$$\mathcal{R}_n(\rho) = \frac{(\rho^2 + a^2)^2 P_\rho^2(\rho)}{2\nu a^2 E^2 R^2} = 1 - b^2 \left(1 + \frac{a^2}{\rho^2 \nu} \right) - \mathcal{F}_n(\rho)(1 + b)^2 \quad (5.24)$$

where we introduced the impact parameter

$$b = \frac{P_y}{E} \quad (5.25)$$

The critical equations

$$\mathcal{R}(\rho) = \mathcal{R}'(\rho) = 0 \quad (5.26)$$

can be written in the form

$$\begin{aligned} a^2 [2 - 2\mathcal{F}_n(\rho_c) - \rho_c \mathcal{F}'_n(\rho_c)]^2 - 8\nu \rho_c^3 \mathcal{F}'_n(\rho_c) &= 0 \\ b_c &= \frac{2 - 2\mathcal{F}_n(\rho_c) - \rho_c \mathcal{F}'_n(\rho_c)}{2 + 2\mathcal{F}_n(\rho_c) + \rho_c \mathcal{F}'_n(\rho_c)} \end{aligned} \quad (5.27)$$

¹²The metric is asymptotically conformally AdS with radius $\ell = \sqrt{L_1 L_5} = L$.

¹³ Photon orbits with non-trivial angular momentum P_ψ exists and were studied in [23].

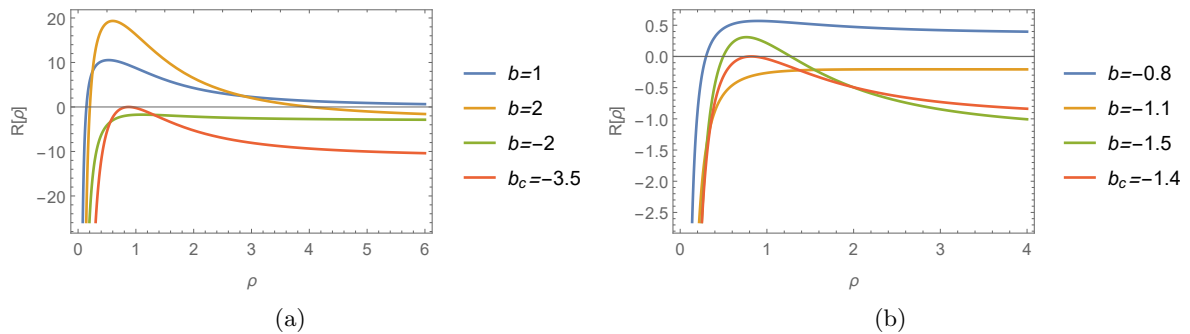


Figure 9: Radial function $\mathcal{R}(\rho)$ as a function of b and ρ for a) $\nu = 4$ and b) $\nu = 10$.

The first equation is quadratic in ν , since \mathcal{F}_n is linear in ν , and we can solve it as a function of ρ_c . The second equation determines $b_c(\rho_c)$ once ν is replaced by $\nu(\rho_c)$ inside \mathcal{F}_n . One finds non trivial solutions for $n \geq 2$. The explicit form of the solutions are not particularly illuminating, so we will not display it here.

In figure 8 we show the curves $b_c(\rho_c)$ and $\nu(\rho_c)$ for $n = 2$. First, we notice that there is no solution in the scattering region $|b| < 1$ where motion is allowed from infinity, so critical geodesics exists but they cannot be reached starting from infinity. Second we observe that for $b \approx \pm 1$, equations (5.27) admit critical solutions for

$$\begin{aligned}
 b_c \approx 1 \quad , \quad \nu \approx \nu_{\min} = \frac{1}{2} + \frac{1}{2} \sqrt{\frac{n+1}{n}} \quad , \quad \rho_c \gg a \\
 b_c \approx -1 \quad , \quad \nu \gg 1
 \end{aligned}
 \tag{5.28}$$

For $\nu < \nu_{\min}$ no critical geodesics exists. We find that geodesics fall into two different categories: scattered geodesics impinging from infinity and finding at most one turning point (green region), and stable orbits confined in the interior of AdS (grey regions) bouncing between two turning points.

This behavior is shown in figure 9, where we draw the radial function $\mathcal{R}(\rho)$ for different values of the impact parameter b . For values of b in the green region the particle comes from infinity and reaches a turning point when $\mathcal{R}(\rho_T) = 0$ (e.g. blue curves in plot (a) and (b)), for values of b in the grey region the particle bounces back and forth between two turning points (orange curve in (a), green curve in (b)).

We conclude that the photon-sphere of fuzzballs in the class $(1, 0, n)$ under study cannot be reached by geodesics scattered from the AdS boundary at infinity.

6 Discussion and outlook

We have studied geodesics for massless neutral probes around the photon-sphere, discriminating between the scattering and absorption phases of asymptotically AdS Kerr-Newman BH and fuzzball geometries. We have found that geodesics near the photon-sphere exhibit always a chaotic behaviour characterised by an exponential growth of the angular dispersion of nearby geodesics. We have computed the critical impact parameters and the

Lyapunov exponent λ governing the exponential growth as functions of the radius of the limiting photon orbits. We have related the Lyapunov exponent λ to the ratio between the vanishing radial velocity and the distance from the photon-sphere

$$\dot{r} \approx 2\lambda(r - r_c) \quad \text{as} \quad r \approx r_c \quad (6.1)$$

The coefficient λ depends on the parameters characterizing the BH: mass, charges and angular momentum. Geodesics with impact parameters below the critical values fall into the horizon with vanishing radial velocities again proportional to the distance from the horizon, with the ratio λ_H given solely in terms of the BH temperature $\lambda_H = 2\pi T$.

The critical exponent λ_H has been recently related to the Lyapunov exponent computing the exponential growth of out-of-time ordered correlators in the quantum mechanic systems describing holographically the near horizon BH geometry [3]. A quantum system dual to a BH is expected to be maximally chaotic, so λ_H has been proposed as an upper bound on quantum chaos a thermal theory at temperature T can develop. The BH photon-sphere is far away from the horizon, so chaos in the photon-sphere is not related to that in the quantum mechanics in any obvious way. Still it is interesting to observe that λ is typically below the advocated upper bound λ_H , but the bound is badly violated inside a very narrow window near extremality, where the BH temperature T_H is very small or vanishing and the photon-sphere coalesces with the BH horizon. Due to the obvious limitations of our classical analysis, we cannot exclude that the violation of the bound could be attributed to quantum effects at low temperatures. Another possibility is that the bound $\lambda < \lambda_H$ should be revised/reconsidered in near extreme conditions even after including quantum or stringy corrections¹⁴

In arbitrary space-time dimension d , we have found instead that λ is bounded by

$$\lambda < \lambda_b = \frac{\sqrt{d-3}}{2b_c} \quad (6.2)$$

with b_c the minimal impact parameter that a massless particle can travel without falling into the BH.

Finally we have considered null geodesics in fuzzball geometries of the so called $(1, 0, n)$ class [15, 29], with asymptotically flat or $AdS^3 \times S^3$ geometries. We have shown that critical photon orbits exists in both cases, but they can be reached from infinity only in the asymptotically flat case. We have also found that the critical exponent λ of the fuzzball is typically smaller than the one of the corresponding BH. This suggests that fuzzball can be distinguished from BH's by the signature of the quasi-normal modes characterising the response of the geometry to small perturbations, that are known to be dominated at late times by a basic mode with time scale given by the inverse of λ [2]. One should however keep in mind that the geometries we have considered correspond to a very special class of somewhat atypical BH micro-states. Further investigation is necessary before reaching a convincing conclusion.¹⁵

¹⁴in particular, the ‘quantisation’ imposed by consistent angular motion, discussed in the Appendix, at the quantum level may lead to a ‘quantisation’ of r_c . We thank G. Festuccia for suggesting this possibility.

¹⁵We would like to thank the referee for raising this point.

Since the scattering processes under study here can be related to out-of-time-order correlators in the boundary theory (at ‘radial’ infinity), one expects that the chaotic behaviour of geodesics reflects into an exponential growth of the correlators in the boundary theory (at ‘radial’ infinity) with Lyapunov exponent λ . High energy scattering in AdS has been also related to correlators involving the insertion of two massless (light-like separated) states (the incoming and outgoing rays) and two heavy states (the BH) in the boundary theory [30]. The time delay and deflection angles experienced by the geodesics measure the derivatives of the (eikonal) phase shift (encoding the relevant part of the correlator) with respect to the energy and angular momentum and determine the location of its poles in coordinate space [31]. One may expect that the results here may provide a detailed prediction about the location of poles in the phase shift of the dual correlators at strong coupling. A complementary picture of the exponential fall off of thermal correlators at large imaginary frequency was obtained in [32] from the study of space-like geodesics probing regions inside the BH horizon. It would be interesting to explore similar connections in the vicinity of the photon-sphere.

A Integrating the angular motion

A different source of chaotic, or more precisely quasi-periodic, behaviour lies in the angular dependence of the metric (2.1). In order to address the existence of such behaviour we investigate the relation between the two angular variables ϕ and θ .

Being interested in critical geodesics, we know that the angular variable θ is constrained by the values $\pm\chi_p$ as shown in section (2.4).

For the non rotating BH’s (*i.e.* $a = 0$) one gets

$$\Theta(\chi) = -b^2\chi^2 + b^2 - \zeta^2 = -b^2(\chi^2 - \chi_p^2) \quad (\text{A.1})$$

with

$$\chi_p^2 = 1 - \frac{\zeta^2}{b^2} \quad (\text{A.2})$$

The motion in the ϕ -direction is given by

$$\Delta\phi = \int_{-\chi_p}^{\chi_p} \frac{\zeta b^{-1} d\chi}{(1 - \chi^2)\sqrt{(\chi + \chi_p)(\chi - \chi_p)}} = \pi + 2\pi n \quad (\text{A.3})$$

As one would expect for critical geodesics in static BH’s, while $\cos\theta$ sweeps the interval $[-\chi_p, \chi_p]$ back and forth, the angle ϕ spans its whole 2π domain (an integer number of times) and the particle trajectory is a full circle.

Rotating BH’s entail a way more complicated relation between θ and ϕ

$$\Delta\phi = i \int_{-\chi_p}^{\chi_p} \frac{d\chi}{\sqrt{1 - \frac{b^2}{\ell^2}}} \left(\frac{1 + \frac{\zeta}{a}}{1 - \chi^2} - \frac{1 + \frac{a\zeta}{\ell^2}}{1 - \frac{a^2}{\ell^2}\chi^2} \right) \frac{1}{\sqrt{(\chi^2 - \chi_p^2)(\chi^2 - \chi_m^2)}} \quad (\text{A.4})$$

The integral can be expressed in terms of (in)complete elliptic integral of the third kind

$$\Pi(n = h^2 | m = k^2) = \int_0^1 \frac{d\chi}{(1 - n\chi^2)\sqrt{(1 - \chi^2)(1 - m\chi^2)}}, \quad (\text{A.5})$$

leading to

$$\Delta\phi = \frac{2i \left[\left(1 + \frac{\zeta}{a}\right) \Pi(n_1|k) - \left(1 + \frac{a\zeta}{\ell^2}\right) \Pi(n_2|k) \right]}{\sqrt{\chi_m^2} \sqrt{1 - \frac{b^2}{\ell^2}}} \quad (\text{A.6})$$

with

$$m = k^2 = \frac{\chi_p^2}{\chi_m^2}, \quad n_1 = h_1^2 = \chi_p^2, \quad n_2 = h_2^2 = \frac{a^2}{\ell^2} \chi_p^2 \quad (\text{A.7})$$

In the case of interest for us $m = k^2 < 0$. In order to have periodic motion one should require

$$\Delta\phi = \pi + 2\pi n$$

this imposes stringent constraints on r_c that are not generically satisfied. As a result, classical motion in the angular variables (for critical radii r_c) is non-periodic and as such chaotic / ergodic in the sense that the orbit covers an entire region of the ‘sphere’. At the quantum level, preventing destructive interference is tantamount to imposing the quantisation condition

$$\Delta\phi = \pi + 2\pi n$$

that selects only a finite, yet possibly very large, set of critical radii r_c .

Acknowledgments

We thank Alice Aldi, Roberto Benzi, Donato Bini, Davide Bufalini, Davide Cassani, Dario Consoli, Sergio Ferrara, Guido Festuccia, Maurizio Firrotta, Francesco Fucito, Stefano Giusto, Salvo Mancani, Andrei Parnachev, Massimo Porrati, Rodolfo Russo, Congkao Wen for useful discussions and Guido Festuccia, Stefano Giusto, Juan Maldacena, Andrei Parnachev, Rodolfo Russo for their comments on the manuscript.

References

- [1] H. A. Buchdahl, *General Relativistic Fluid Spheres*, *Phys. Rev.* **116** (1959) 1027.
- [2] V. Cardoso, A. S. Miranda, E. Berti, H. Witek and V. T. Zanchin, *Geodesic stability, Lyapunov exponents and quasinormal modes*, *Phys. Rev.* **D79** (2009) 064016, [[0812.1806](#)].
- [3] J. Maldacena, S. H. Shenker and D. Stanford, *A bound on chaos*, *JHEP* **08** (2016) 106, [[1503.01409](#)].
- [4] S. H. Shenker and D. Stanford, *Black holes and the butterfly effect*, *JHEP* **03** (2014) 067, [[1306.0622](#)].
- [5] S. H. Shenker and D. Stanford, *Multiple Shocks*, *JHEP* **12** (2014) 046, [[1312.3296](#)].
- [6] Y. Kiem, H. L. Verlinde and E. P. Verlinde, *Black hole horizons and complementarity*, *Phys. Rev.* **D52** (1995) 7053–7065, [[hep-th/9502074](#)].
- [7] O. Lunin and S. D. Mathur, *Statistical interpretation of Bekenstein entropy for systems with a stretched horizon*, *Phys. Rev. Lett.* **88** (2002) 211303, [[hep-th/0202072](#)].
- [8] O. Lunin and S. D. Mathur, *AdS / CFT duality and the black hole information paradox*, *Nucl. Phys.* **B623** (2002) 342–394, [[hep-th/0109154](#)].

- [9] S. D. Mathur, *The Fuzzball proposal for black holes: An Elementary review*, *Fortsch. Phys.* **53** (2005) 793–827, [[hep-th/0502050](#)].
- [10] S. D. Mathur, *Fuzzballs and the information paradox: A Summary and conjectures*, [0810.4525](#).
- [11] P. Hintz and A. Vasy, *Analysis of linear waves near the Cauchy horizon of cosmological black holes*, *J. Math. Phys.* **58** (2017) 081509, [[1512.08004](#)].
- [12] S. Hollands, R. M. Wald and J. Zahn, *Quantum Instability of the Cauchy Horizon in Reissner-Nordström-deSitter Spacetime*, [1912.06047](#).
- [13] I. Bena, S. Giusto, R. Russo, M. Shigemori and N. P. Warner, *Habemus Superstratum! A constructive proof of the existence of superstrata*, *JHEP* **05** (2015) 110, [[1503.01463](#)].
- [14] I. Bena, E. Martinec, D. Turton and N. P. Warner, *Momentum Fractionation on Superstrata*, *JHEP* **05** (2016) 064, [[1601.05805](#)].
- [15] I. Bena, S. Giusto, E. J. Martinec, R. Russo, M. Shigemori, D. Turton et al., *Smooth horizonless geometries deep inside the black-hole regime*, *Phys. Rev. Lett.* **117** (2016) 201601, [[1607.03908](#)].
- [16] S. Giusto, J. F. Morales and R. Russo, *D1D5 microstate geometries from string amplitudes*, *JHEP* **03** (2010) 130, [[0912.2270](#)].
- [17] S. Giusto, R. Russo and D. Turton, *New D1-D5-P geometries from string amplitudes*, *JHEP* **11** (2011) 062, [[1108.6331](#)].
- [18] M. Bianchi, J. F. Morales and L. Pieri, *Stringy origin of 4d black hole microstates*, *JHEP* **06** (2016) 003, [[1603.05169](#)].
- [19] M. Bianchi, J. F. Morales, L. Pieri and N. Zinnato, *More on microstate geometries of 4d black holes*, *JHEP* **05** (2017) 147, [[1701.05520](#)].
- [20] I. Bena, D. Turton, R. Walker and N. P. Warner, *Integrability and Black-Hole Microstate Geometries*, *JHEP* **11** (2017) 021, [[1709.01107](#)].
- [21] I. Bena, E. J. Martinec, R. Walker and N. P. Warner, *Early Scrambling and Capped BTZ Geometries*, *JHEP* **04** (2019) 126, [[1812.05110](#)].
- [22] I. Bena, P. Heidmann, R. Monten and N. P. Warner, *Thermal Decay without Information Loss in Horizonless Microstate Geometries*, *SciPost Phys.* **7** (2019) 063, [[1905.05194](#)].
- [23] M. Bianchi, D. Consoli, A. Grillo and J. F. Morales, *The dark side of fuzzball geometries*, *JHEP* **05** (2019) 126, [[1811.02397](#)].
- [24] M. Bianchi, D. Consoli and J. F. Morales, *Probing Fuzzballs with Particles, Waves and Strings*, *JHEP* **06** (2018) 157, [[1711.10287](#)].
- [25] V. Cardoso and P. Pani, *Testing the nature of dark compact objects: a status report*, *Living Rev. Rel.* **22** (2019) 4, [[1904.05363](#)].
- [26] L. Barack et al., *Black holes, gravitational waves and fundamental physics: a roadmap*, *Class. Quant. Grav.* **36** (2019) 143001, [[1806.05195](#)].
- [27] M. M. Caldarelli, G. Cognola and D. Klemm, *Thermodynamics of Kerr-Newman-AdS black holes and conformal field theories*, *Class. Quant. Grav.* **17** (2000) 399–420, [[hep-th/9908022](#)].

- [28] S. Chandrasekhar, *The mathematical theory of black holes*, in *Oxford, UK: Clarendon (1992) 646 p., OXFORD, UK: CLARENDON (1985) 646 P.*, 1985.
- [29] I. Bena, S. Giusto, E. J. Martinec, R. Russo, M. Shigemori, D. Turton et al., *Asymptotically-flat supergravity solutions deep inside the black-hole regime*, *JHEP* **02** (2018) 014, [[1711.10474](#)].
- [30] M. Kulaxizi, G. S. Ng and A. Parnachev, *Black Holes, Heavy States, Phase Shift and Anomalous Dimensions*, *SciPost Phys.* **6** (2019) 065, [[1812.03120](#)].
- [31] R. Karlsson, M. Kulaxizi, A. Parnachev and P. Tadić, *Black Holes and Conformal Regge Bootstrap*, *JHEP* **10** (2019) 046, [[1904.00060](#)].
- [32] G. Festuccia and H. Liu, *Excursions beyond the horizon: Black hole singularities in Yang-Mills theories. I.*, *JHEP* **04** (2006) 044, [[hep-th/0506202](#)].